

Biases on cosmological parameters by general relativity effects

L. Lopez-Honorez¹, O. Mena² and S. Rigolin³¹ *Service de Physique Théorique, Université Libre de Bruxelles, Brussels, Belgium*² *IFIC-CSIC and Universidad de Valencia, Valencia, Spain and*³ *Dipartimento di Fisica, Università di Padova and INFN Padova, Padova, Italy*

General relativistic corrections to the galaxy power spectrum appearing at the horizon scale, if neglected, may induce biases on the measured values of the cosmological parameters. In this paper, we study the impact of general relativistic effects on non standard cosmologies such as scenarios with a time dependent dark energy equation of state, with a coupling between the dark energy and the dark matter fluids or with non-Gaussianities. We then explore whether general relativistic corrections affect future constraints on cosmological parameters in the case of a constant dark energy equation of state and of non-Gaussianities. We find that relativistic corrections on the power spectrum are not expected to affect the foreseen errors on the cosmological parameters nor to induce large biases on them.

PACS numbers:

I. INTRODUCTION

The complete general relativistic description of the observed matter power spectrum is, at large scales, significantly different from the standard Newtonian one. The observed redshift and position of galaxies are affected by matter fluctuations and gravity waves between the source and the observer, see e.g. Ref. [1]. In addition, the matter density perturbation, δ_m , is gauge dependent while observable quantities, such as the power spectrum, should be gauge invariant. The standard picture looks, therefore, incomplete, and a general relativistic description is needed in order to correctly compute the measured observables [2, 3]. Current observations, based on available galaxy surveys, are not affected, in practice, by general relativistic corrections since they appear only at very large scales. In future galaxy surveys, however, these corrections may interfere with the measure of other physical effects which modify the large-scale shape of the power spectrum.

In this paper, we study the general relativistic effects in several cosmological scenarios, like: i) a constant dark energy equation of state; ii) a time varying equation of state $w(a)$; iii) non-Gaussianities; iv) a coupling between dark energy and dark matter; and finally iv) massive neutrinos. For the scenarios i) and iii), we compute the expected errors and biases from a future Euclid-like galaxy survey by means of a Fisher matrix analysis, comparing the results with and without general relativistic corrections in the matter power spectrum.

The structure of the paper is the following. Section II summarizes the general relativistic corrections treatment. In Sec. III the impact of general relativistic corrections in the cosmological scenarios quoted above is presented. The expected errors and biases on the cosmological parameters are computed in Sec. IV for two particular scenarios. Finally in Sec. V we conclude.

II. PRELIMINARIES

Following the results of Refs. [1–5], we briefly summarize the treatment of the observed galaxy power spectrum in redshift space. In linear perturbation theory, the observed (matter) density ρ_m at a given redshift is defined as a function of the density fluctuation δ_m and the background (matter) density $\bar{\rho}_m$

$$\rho_m \equiv \bar{\rho}_m(\bar{z})(1 + \delta_m). \quad (1)$$

For the standard Λ CDM cosmology, that we take as reference, the background matter density in terms of the current Hubble parameter H_0 and today's matter density relative to the critical density Ω_m reads ¹:

$$\bar{\rho}_m(\bar{z}) = \frac{3H_0^2}{8\pi G}\Omega_m(1 + \bar{z})^3. \quad (2)$$

In Eqs. (1) and (2), the dependence of the background density $\bar{\rho}_m$ on the background redshift \bar{z} has been made explicit. The ratio between the emitter and the observed frequencies at the background level is defined as

$$1 + \bar{z} = \frac{\bar{\nu}_e}{\bar{\nu}_o} = \frac{(\bar{K}^\mu \bar{u}_\mu)_e}{(\bar{K}^\mu \bar{u}_\mu)_o} = \frac{1}{\bar{a}}, \quad (3)$$

where \bar{K}^μ and \bar{u}_μ are the background photon wave vector and the background emitter/observer (e/o) four-velocity, respectively. At linear order in perturbation theory, the observed redshift of a given source, z , differs from the background one due to the matter/gravity fluctuations that the photon encounters between the emitter and the observer positions. The perturbed four-velocity and photon null-vector read:

$$u^\mu = \frac{1}{\bar{a}}(1 - A, v^i); \quad (4)$$

$$K^\mu = \frac{\bar{\nu}}{\bar{a}}\left(1 + \frac{\delta\nu}{\bar{\nu}}, n^i + \delta n^i\right), \quad (5)$$

where $\mu = 0, \dots, 3$ and $i = 1, \dots, 3$. v^i is the peculiar velocity of the observer/emitter and $\delta\nu$ and δn^i are the perturbed photon frequency and propagation direction, respectively. The conventions used for the perturbed Friedmann-Robertson-Walker (FRW) metric, together with a list of useful relations, can be found in Appendix A. The observed (perturbed) redshift z thus reads:

$$1 + z \equiv 1 + \bar{z} + \delta z = \frac{(K^\mu u_\mu)_e}{(K^\mu u_\mu)_o} = (1 + \bar{z}) \left[1 + \left(\frac{\delta\nu}{\bar{\nu}} + A + (B_i - v_i) n^i \right)_e \right]. \quad (6)$$

Expressing the matter density in terms of the observed redshift, instead of the unobservable background one, it gives:

$$\rho_m = \bar{\rho}_m(z) \left(1 + \delta_m - \frac{d\bar{\rho}_m}{dz} \frac{\delta z}{\bar{\rho}_m} \right) \equiv \bar{\rho}_m(z) (1 + \Delta_z), \quad (7)$$

with the background matter density $\bar{\rho}_m(z)$ function of the observed redshift z . While the density contrast δ_m and the redshift fluctuation δz are gauge dependent quantities, their combination Δ_z is, instead, gauge invariant. Notice, however, that the truly observed quantity is the galaxy number density perturbation [2, 4, 5] corresponding to:

$$\Delta_{obs} = \frac{\delta N}{\bar{N}} \equiv \frac{N(z) - \bar{N}(z)}{\bar{N}(z)} = \Delta_z + \frac{\delta \text{Vol}}{\bar{\text{Vol}}}, \quad (8)$$

where an extra contribution from the physical survey volume perturbation appears. Being the volume density perturbation, δVol , a gauge invariant quantity, Δ_{obs} is automatically gauge invariant, as it should be for any observable quantity. In addition, one has to introduce a bias between galaxy and matter overdensities. We will ignore for the moment the bias issue, deferring a brief discussion of this aspect to Sec. III B.

Making use of the null energy condition and the photon geodesic equation (see Appendix A and also Refs. [1–4, 6] for more details) one can write Δ_z in terms of gauge invariant quantities as:

$$\Delta_z = \Delta_m + 3\mathbf{n} \cdot \mathbf{V} + 3(\Psi_B - \Phi_B) - 3 \int_{\lambda_o}^{\lambda_s} d\lambda (\dot{\Psi}_B - \dot{\Phi}_B), \quad (9)$$

¹ See Sec. III C for non standard cosmologies in which Eq. (2) is not valid.

where Φ_B and Ψ_B are the Bardeen potentials and Δ_m and \mathbf{V} are the gauge invariant matter density contrast and peculiar velocity, which definitions can be found in Appendix A. The last term in Eq. (9) is the usual integrated Sachs–Wolfe effect between the observer and the emission point with $d/d\lambda = \partial_\tau + n^i \partial_i$. The survey volume perturbation δVol has been carefully derived in several references, see e.g. Refs. [2, 4], we therefore omit the details of its calculation here. Neglecting the unmeasurable monopole and dipole perturbations at the observer position, the expression of Δ_{obs} in terms of gauge invariant quantities reads:

$$\begin{aligned} \Delta_{obs} = & \Delta_m + \Psi_B - \Phi_B - \mathbf{n} \cdot \mathbf{V} - \frac{1}{\mathcal{H}} \left[n^i \partial_i \Psi_B + \dot{\Phi}_B + \frac{d}{d\lambda} (\mathbf{n} \cdot \mathbf{V}) \right] \\ & + \left(\frac{2}{r_s \mathcal{H}} + \frac{\dot{\mathcal{H}}}{\mathcal{H}^2} \right) \left[\mathbf{n} \cdot \mathbf{V} + \Psi_B + \int_0^{r_s} d\lambda (\dot{\Psi}_B - \dot{\Phi}_B) \right] \\ & + \frac{2}{r_s} \int_0^{r_s} d\lambda (\Psi_B - \Phi_B) - \frac{1}{r_s} \int_0^{r_s} d\lambda \frac{r_s - r}{r} \Delta_\Omega (\Psi_B - \Phi_B) , \end{aligned} \quad (10)$$

where $r_s = \int_{\tau_o}^{\tau_s} d\tau$ corresponds to the comoving distance between the source and the observer and Δ_Ω is the angular Laplacian on a unit sphere. Notice that Eq. (10) holds for the standard cosmology case and reduces to Eq. (30) of Ref. [4] once the Euler equation for the gauge invariant matter velocity scalar perturbation:

$$\dot{V}^i = -\mathcal{H}V^i - \partial^i \Psi_B , \quad (11)$$

is implemented. Also, let us emphasize that we have assumed a constant comoving source number density and ignored the vector and tensor contributions in Eqs. (9) and (10).

For later convenience, let us express Eqs. (9) and (10) in the Newtonian gauge. The density perturbations Δ_z and Δ_{obs} read respectively:

$$\Delta_z = \delta_m^N + 3 \mathbf{n} \cdot \mathbf{v} + 3\Psi_N - 3 \int d\lambda (\dot{\Psi}_N + \dot{\Phi}_N) ; \quad (12)$$

$$\begin{aligned} \Delta_{obs} = & \delta_m^N + \frac{1}{\mathcal{H}} \mathbf{n} \cdot \partial_r \mathbf{v} - 2\kappa + \Psi_N - 2\Phi_N + \frac{1}{\mathcal{H}} \dot{\Phi}_N \\ & + \left(\frac{2}{r_s \mathcal{H}} + \frac{\dot{\mathcal{H}}}{\mathcal{H}^2} \right) \left[\mathbf{n} \cdot \mathbf{v} + \Psi_N + \int_0^{r_s} d\lambda (\dot{\Psi}_N + \dot{\Phi}_N) \right] + \frac{2}{r_s} \int_0^{r_s} d\lambda (\Psi_N + \Phi_N) , \end{aligned} \quad (13)$$

where κ is the lensing convergence (see Eq. (A16)), Ψ_N and Φ_N are the scalar perturbations of the metric in the Newtonian gauge (see Appendix A) and the partial derivative $\partial_r = e_r^i \partial_i = -n^i \partial_i$ with e_r^i indicating the source position. With δ_m^N and \mathbf{v} , we refer to the matter density and peculiar velocity perturbation in the Newtonian gauge.

In the standard Newtonian approximation, the galaxy number density perturbation, Δ_{st} , only gets contributions from the three first terms of Eq. (13), namely from the matter density perturbation, the redshift space distortion term and from the convergence term. We consider that, neglecting the bias between galaxy and matter overdensities, the associated standard Newtonian power spectrum is related to the matter power spectrum evaluated in the synchronous gauge² in the following way:

$$P_{\Delta_{st}} = P_m^S (1 + f_{\text{eff}} \mu_k^2)^2 . \quad (14)$$

The latter is typically used for calculating the power spectrum when relativistic contributions can be safely neglected (i.e. for scales much smaller than the horizon scale). In Eq. (14), the index S refers to the synchronous comoving gauge, f_{eff} is the linear growth function and μ_k is the cosine of the angle between the line of sight and the wave vector k . In standard cosmological scenarios, the growth function f_{eff} is given by $d \ln \delta_m / d \ln a$.

Notice that in Eq. (14) we have ignored the contribution from the convergence term. Through all this study contributions from projected quantities have been neglected when computing the 3-D power spectrum

² For a comprehensive discussion see for example Refs. [5, 6].

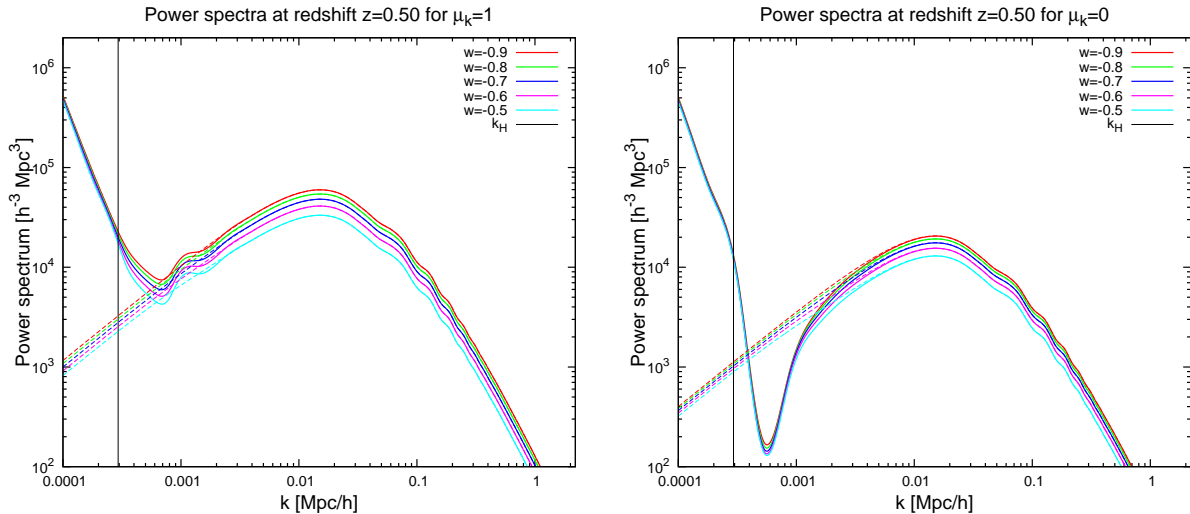


FIG. 1: $P_{\Delta_{obs}}(k)$ (solid lines) and $P_{\Delta_{st}}(k)$ (dashed lines) for $\mu_k = 1$ (left panel) and $\mu_k = 0$ (right panel). The dark energy equation of state w is assumed to be constant and has been varied between -0.9 and -0.5 . The vertical line corresponds to the horizon scale k_H for $w = -0.9$.

$P(k)$, while their contributions have been accounted for when calculating the 2-D angular power spectrum C_ℓ . Also, given that we expect galaxy formation to proceed in the potential wells of dark matter halos³, all the computed power spectra ($P(k)$ or C_ℓ) in the following will correspond to the dark matter power spectra which have been obtained using the available public version of CAMB [8].

III. COSMOLOGICAL SCENARIOS

We explore below the impact of general relativistic corrections in several cosmological scenarios which include the presence of a constant dark energy equation of state and the presence of non-Gaussianities. In the next section, we will estimate the foreseen errors on the several cosmological parameters involved in each of these two cosmologies using the Fisher matrix formalism. For the sake of illustration, we also discuss the effect of general relativistic corrections on the observed galaxy power spectrum in the case of a time varying equation of state $w(a)$, a coupling between dark energy and dark matter and massive neutrinos.

Unless otherwise stated, the following numerical values for the cosmological parameters have been used: $\Omega_b h^2 = 0.02267$, $\Omega_{dm} h^2 = 0.1131$, $h = 0.705$, the scalar amplitude $A_s = 2.64 \times 10^{-9}$ and the scalar spectral index $n_s = 0.96$. $\Omega_{b(dm)}$ refers to the current baryon (dark matter) energy density relative to the critical density and h is related to the present value of the Hubble parameter $H_0 = 100h$ Mpc/km/s. The sound speed for the dark energy fluid is fixed to $c_s^2 = 1$.

A. Dark energy

We first consider a cosmological model including standard cold dark matter and a dark energy fluid characterized by a constant equation of state w . Figure 1 shows the dark matter power spectra $P_{\Delta_{obs}}(k, \mu_k)$ and $P_{\Delta_{st}}(k, \mu_k)$ for both the line-of-sight ($\mu_k = 1$) and the transverse ($\mu_k = 0$) modes at $z = 0.5$ for several values of w , ranging from $w = -0.9$ to $w = -0.5$. The horizon scale, k_H is also shown for the $w = -0.9$ case.

³ We know that luminous red galaxies occupy massive dark matter halos today from weak lensing measurements [7].

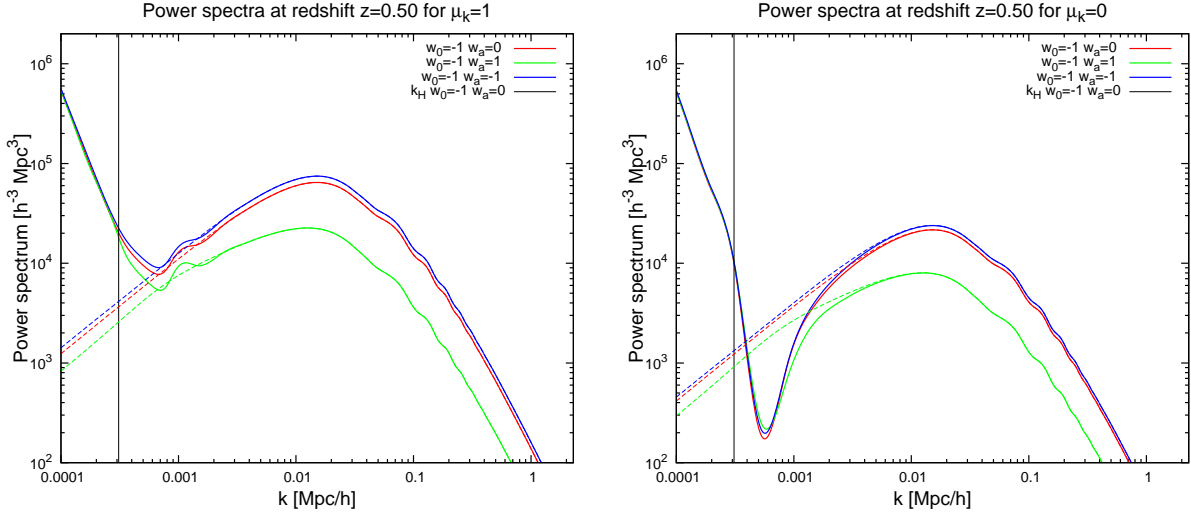


FIG. 2: $P_{\Delta_{obs}}(k)$ (solid lines) and $P_{\Delta_{st}}(k)$ (dashed lines) for $\mu_k = 1$ (left panel) and $\mu_k = 0$ (right panel) for the three possible $w(a)$ cosmologies explored here at $z = 0.5$. The vertical lines depict the horizon scale k_H for $w_0 = -1$ and $w_a = 0$.

Notice that, in Sec. IIID, we discuss the k position of the dip appearing at large scales in the power spectrum $P_{\Delta_{obs}}(k, \mu_k)$ in the transverse direction (right plot). The modifications in the shape of the power spectra when relativistic effects are considered barely change when the dark energy equation of state is varied. In addition, the new features on the power spectrum induced by the general relativity terms appear only at very large scales: consequently, one would not expect much improvement on the measurement of w when relativistic effects are included. For the same reason, the bias induced on the dark energy equation of state w when the data are fitted to $P_{\Delta_{st}}$ (instead of using the full description given by $P_{\Delta_{obs}}$) is expected to be negligible. In Sec. IV, we estimate the foreseen errors on several cosmological parameters within a constant dark energy equation of state cosmological scenario using the Fisher matrix formalism.

We also consider a time varying equation of state with a parameterization that has been extensively explored in the literature [9–12]: $w(a) = w_0 + w_a(1 - a)$. We study 3 cases: i) $w_0 = -1$ and $w_a = 0$; ii) $w_0 = -1$ and $w_a = 1$; iii) $w_0 = -1$ and $w_a = -1$. For our numerical calculations, we have used the Parameterized Post-Friedmann (PPF) prescription for the dark energy perturbations, see Refs. [13–15].

Figure 2 shows the standard Newtonian matter power spectrum and the one with relativistic corrections included for the three $w(a)$ cosmologies above, for both the line of sight and the transverse modes at redshift $z = 0.5$. Notice that the dependence of the general relativistic corrections on the time varying equation of state $w(a)$ is as mild as for the case of constant w . The new features due to general relativistic corrections in the line of sight modes barely change when different values of w_0 and w_a are considered. Therefore, the extra information contained in these general relativistic terms will poorly increase the precision on the measurement of a time varying dark energy equation of state.

B. Non-Gaussianity

In this section, we take into account a non zero bias between galaxy and dark matter overdensities. Following the prescription of several recent studies [5, 6, 16] and considering a linear bias relation in the comoving synchronous gauge, the galaxy and dark matter overdensities are related by $\delta_g^S = b \delta_{dm}^S$. If the primordial fluctuations are Gaussian, it is generally assumed that this bias b is scale independent.

Deviations from Gaussian initial conditions offer a unique tool for testing the mechanism which generated primordial perturbations. Non-Gaussianities are commonly characterized by a single parameter, f_{NL} . The local primordial Bardeen gauge-invariant potential on large scales in the matter dominated era can be written

as [17–20]

$$\Phi_{\text{NG}} = \Phi_G + f_{\text{NL}} (\Phi_G^2 - \langle \Phi_G^2 \rangle) , \quad (15)$$

where Φ_G is a Gaussian random field. The non-Gaussianity parameter f_{NL} is often considered to be a constant, yielding non-Gaussianities of the *local* type with a bispectrum which is maximized for squeezed configurations [21]. The standard observables to constrain non-Gaussianities are the CMB and the Large-Scale Structure (LSS) of the Universe. References [22] and [23] showed that primordial non-Gaussianities affect the clustering of dark matter halos inducing a scale-dependent large-scale bias [24–30].

Following Refs. [22, 24, 31] (see also [6, 16, 32] for recent studies with general relativity corrections), we consider a scale dependent bias induced by the local non-Gaussianity of the following form

$$\delta_g^S = b \delta_{\text{dm}}^S \quad \text{where} \quad b = b_G + \Delta b , \quad (16)$$

with b_G , a constant Gaussian bias and

$$\Delta b = 3f_{\text{NL}}(1 - b_G)\delta_c \frac{H_0^2 \Omega_m}{k^2 T(k) D(a)} . \quad (17)$$

$T(k)$ is the linear transfer function that we have taken to be equal to unity and $D(a)$ is the growth factor defined as $\delta_{\text{dm}}(a)/\delta_{\text{dm}}(a=1)$. The linear overdensity for spherical collapse can be considered as a constant: $\delta_c = 1.686$ [33].

The resulting non Gaussian halo power spectrum is shown in Fig. 3. The standard Newtonian power spectrum is now obtained using

$$P_{\Delta_{st}} = P_{\text{dm}}^S (b_G + \Delta b + f_{\text{eff}} \mu_k^2)^2 , \quad (18)$$

while the general relativity-corrected power spectra is obtained expressing Eq. (10) in the synchronous gauge and replacing δ_m by the galaxy density fluctuation defined in Eq. (16). The left (right) panel of Fig. 3 shows the power spectra for the line of sight (transverse) modes. Note that even in the absence of general relativity corrections the introduction of a negative f_{NL} induces the presence of a dip at large scales (contrarily to the case of positive f_{NL}). This can be easily understood by studying the k dependence of the factor multiplying P_{dm}^S in Eq. (18). In the negative f_{NL} case, once we introduce general relativity corrections, the dip at large scales can become shallower (deeper) in the $\mu_k = 1$ ($\mu_k = 0$) case. In the case of the positive f_{NL} values considered here, the presence of non Gaussianities induces an increase of the Newtonian matter power spectrum at $k < 0.01$ Mpc/ h . General relativity corrections may also induce an increase of the power spectrum but at larger scales, $k < 0.001$ Mpc/ h . However, non-Gaussianities dominate the shape of the power spectrum and make the general relativity effects totally subdominant. The shape of the non-Gaussian power spectrum barely changes when general relativistic effects are considered, regardless of the sign of the non Gaussianity parameter f_{NL} . Therefore, we do not expect an important improvement on the precision measurement of the different cosmological parameters nor large biases on them in a non-Gaussianity scenario when general relativity corrections are included, see Sec. IV for a quantitative analysis.

C. Coupled and modified gravity cosmologies

Interactions within the dark sectors, i.e. between cold dark matter and dark energy, are still allowed by observations [34–50]. Constraints on coupled cosmologies as well as on modified gravity models could also be affected by the relativistic effects on the matter power spectrum. As an illustration, we parameterize the dark matter-dark energy interactions at the level of the stress-energy tensor conservation equations. Following the notations of [47], an energy momentum exchange of the following form can be introduced:

$$\nabla_\mu T_{(\text{dm})\nu}^\mu = Q_\nu \quad \text{and} \quad \nabla_\mu T_{(\text{de})\nu}^\mu = -Q_\nu , \quad (19)$$

with

$$Q_\nu = \xi \mathcal{H} \rho_{\text{de}} u_\nu^{\text{dm}} / a \quad \text{or} \quad Q_\nu = \xi \mathcal{H} \rho_{\text{de}} u_\nu^{\text{de}} / a , \quad (20)$$

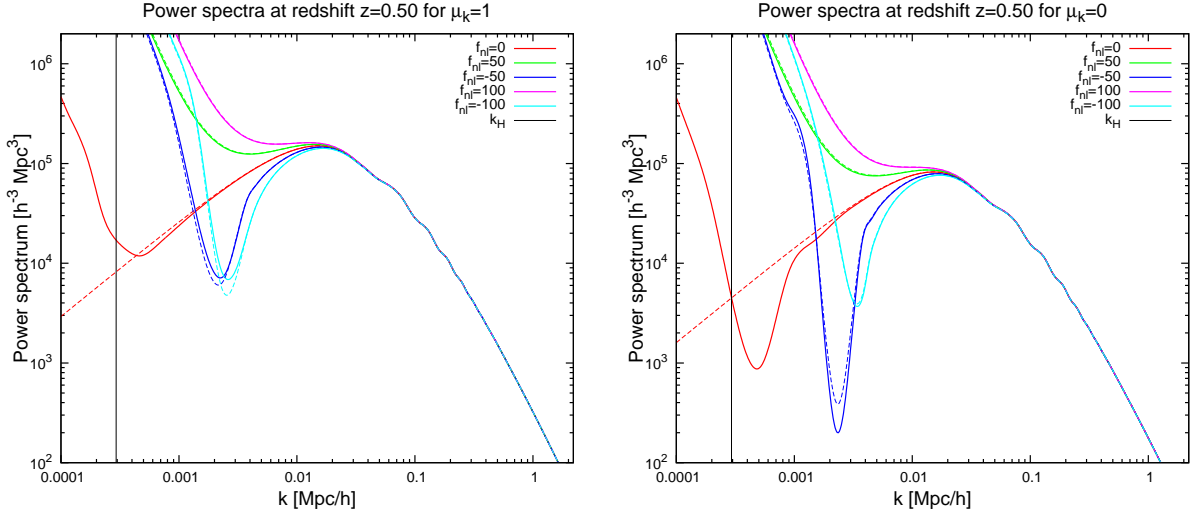


FIG. 3: $P_{\Delta_{obs}}(k)$ (solid lines) and $P_{\Delta_{st}}(k)$ (dashed lines) for $\mu_k = 1$ (left) and $\mu_k = 0$ (right) for five different values of the parameter f_{NL} , for a Gaussian bias $b_G = 2$ and $z = 0.5$. The vertical lines depict the horizon scale k_H for $w = -0.9$.

where $u_\nu^{\text{dm(de)}}$ is the cold dark matter (dark energy) four velocity and ξ is a dimensionless coupling, considered negative in order to avoid early time non adiabatic instabilities [43]. In general, coupled models with Q_ν proportional to u_ν^{de} are effectively modified gravity models. Assuming a flat universe and perfect measurements of $\Omega_{\text{dm}}h^2$, $\Omega_{\text{b}}h^2$, and of the angular diameter distance to the last scattering surface from Cosmic Microwave Background (CMB) observations [51], the amplitude of ξ is degenerate with the physical energy density in dark matter today, $\Omega_{\text{dm}}h^2$. Consequently, $\Omega_{\text{dm}}h^2$ should be changed accordingly each time ξ is varied, see Appendix B of Ref. [48] for the values of $\Omega_{\text{dm}}h^2$ and h considered here.

Coupled cosmologies imply some extra terms in the expression of the gauge invariant matter fluctuation Eq. (9). Indeed, in the case of the coupled models studied here

$$\frac{d\rho_{\text{dm}}}{dz} = 3\frac{\rho_{\text{dm}}}{1+z} - \xi\frac{\rho_{\text{de}}}{1+z}, \quad (21)$$

which directly affects the expressions for Δ_m and Δ_z . In the u_ν^{dm} case the gauge invariant quantity defined in Eq. (7) becomes:

$$\Delta_z^{u_\nu^{\text{dm}}} = \Delta_{\text{dm}}^\xi + \left(3 - \xi\frac{\rho_{\text{de}}}{\rho_{\text{dm}}}\right) \left[\mathbf{n} \cdot \mathbf{V}_{\text{dm}} + (\Psi_B - \Phi_B) + \int_0^{r_s} d\lambda (\dot{\Psi}_B - \dot{\Phi}_B) \right], \quad (22)$$

where we have made explicit the ξ dependence of the gauge invariant dark matter density perturbation:

$$\Delta_{\text{dm}}^\xi = \delta_{\text{dm}} + (3 - \xi\rho_{\text{de}}/\rho_{\text{dm}})\mathcal{R}/\mathcal{H}, \quad (23)$$

where \mathcal{R} is the curvature perturbation defined in Eq. (A5). In the u_ν^{de} case another extra contribution results from the modified Euler equation. In the gauge invariant formalism for dark matter perturbations (see e.g. [47])

$$\dot{\mathbf{V}}_{\text{dm}} = -\mathcal{H}\mathbf{V}_{\text{dm}} - \nabla\Psi_B + \xi\frac{\rho_{\text{de}}}{\rho_{\text{dm}}}\mathcal{H}(\mathbf{V}_{\text{de}} - \mathbf{V}_{\text{dm}}). \quad (24)$$

Therefore, the perturbation in the number density of galaxies in the u_ν^{de} case reads

$$\Delta_z^{u_\nu^{\text{de}}} = \Delta_z^{u_\nu^{\text{dm}}} - \xi\frac{\rho_{\text{de}}}{\rho_{\text{dm}}}(\mathbf{V}_{\text{de}} - \mathbf{V}_{\text{dm}}) \cdot \mathbf{n}. \quad (25)$$

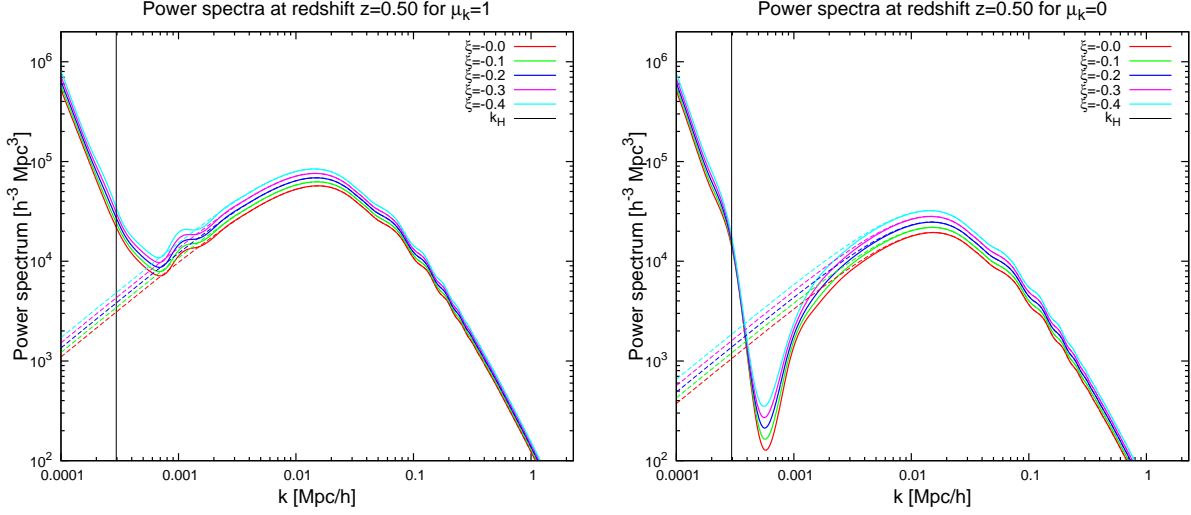


FIG. 4: The left (right) panel depicts $P_{\Delta_{obs}}(k)$ and $P_{\Delta_{st}}(k)$ by solid and dashed lines, respectively for coupled models $\propto u_\nu^{\text{dm}}$ and $\mu_k = 1$ ($\mu_k = 0$). Different values of the coupling ξ are illustrated, and the redshift is $z = 0.5$. In all the models, the cosmological parameters $\Omega_{\text{dm}}h^2$ and h have been chosen to satisfy CMB constraints. The vertical lines show the horizon scale for $w = -0.9$.

Figure 4 depicts the resulting matter power spectra $P_{\Delta_{obs}}(k, \mu_k)$ and $P_{\Delta_{st}}(k, \mu_k)$ for coupled models with an interaction term proportional to u_ν^{dm} for both the line of sight and transverse modes at $z = 0.5$ and for different values of the coupling ξ . Notice that in coupled cosmological scenarios considered here, the growth function appearing in the definition of $P_{\Delta_{st}}(k, \mu_k)$ in Eq. (14) is given by $d \ln \delta_{\text{dm}} / d \ln a + \xi \rho_{\text{de}} / \rho_{\text{dm}}$ [48]. Similar results are obtained for the case in which the coupling term is proportional to u_ν^{de} . As in the case of the dark energy equation of state, no strong biases are expected in constraining the coupling when these new general relativistic terms are included in the analysis: the shape of the different curves including relativistic corrections barely changes when the coupling is varied.

D. Neutrino masses

Consider a Λ CDM model plus massive neutrinos of a given energy density $\Omega_\nu h^2$. We would like to determine if the massive neutrino energy density could affect the position of the dip appearing in the dark matter power spectrum $P_{\Delta_{obs}}(k, \mu_k)$ for the transverse modes ($\mu_k = 0$). In order to simplify the discussion let us consider the expression of Δ_{obs} in the Newtonian gauge, see Eq. (13). In the approximation in which all projected quantities in the power spectrum computation are neglected, the dip appears for $\mu_k = 0$ (i.e. $\mathbf{n} \cdot \mathbf{v} = 0$) when the condition

$$\delta_{\text{dm}}^N + \Psi_N - 2\Phi_N + \frac{1}{\mathcal{H}} \dot{\Phi}_N + \left(\frac{2}{r_s \mathcal{H}} + \frac{\dot{\mathcal{H}}}{\mathcal{H}^2} \right) \Psi_N = 0 \quad (26)$$

is satisfied. For a specific choice of redshift and of cosmology, the factor $\Sigma = (2/(r_s \mathcal{H}) + \dot{\mathcal{H}}/\mathcal{H}^2)$ does not depend on the wave number k . Neglecting anisotropic stress, so that $\Psi_N = \Phi_N$, and making use of the Einstein equations (see Ref. [52] for the prescription used here):

$$k^2 \Psi_N = -\frac{3}{2} \mathcal{H}^2 \sum_a \Omega_a \left(\delta_a^N + 3 \frac{\mathcal{H}}{k} (1 + w_a) v_a \right), \quad (27)$$

$$k^2 (\dot{\Phi}_N + \mathcal{H} \Psi_N) = \frac{3}{2} \mathcal{H}^2 \sum_a \Omega_a (1 + w_a) k v_a, \quad (28)$$

the dip position in the Fourier space as a function of Ω_a, δ_a, v_a can be extracted:

$$k^2 = \frac{3}{2\delta_{\text{dm}}}\mathcal{H}^2 \sum_a \Omega_a \left[(\Sigma - 2)\delta_a + (w_a + 1)v_a \left(3\frac{\mathcal{H}}{k}(\Sigma - 2) - \frac{k}{\mathcal{H}} \right) \right]. \quad (29)$$

In the previous equations the index a runs over all the relevant fluids. In principle, different scenarios with different Ω_ν will show a dip at different wave numbers. However, this k difference will vanish when the total matter energy density (i.e. cold dark matter plus baryons plus the neutrino contribution) is kept constant. Therefore, general relativity effects can not help in extracting the values of the neutrino masses.

IV. COSMOLOGICAL PARAMETER FORECASTS AND BIASES

In this section we explore if the measurement of the different cosmological parameters is affected by relativistic corrections. We present constraints from future galaxy survey measurements, making use of the Fisher matrix formalism. Then, we compare the cosmological parameter errors with and without general relativistic corrections.

A. Methodology

The Fisher matrix is defined as the expectation value of the second derivative of the likelihood surface about the maximum. As long as the posterior distribution for the parameters is well approximated by a multivariate Gaussian function, its elements are given by [53–55]

$$F_{\alpha\beta} = \frac{1}{2}\text{Tr} [C^{-1}C_{,\alpha}C^{-1}C_{,\beta}] , \quad (30)$$

where $C = S+N$ is the total covariance which consists of signal S and noise N terms. The commas in Eq. (30) denote derivatives with respect to the cosmological parameters within the assumed fiducial cosmology. The $1-\sigma$ error on a given parameter p_α marginalized over the other parameters is $\sigma(p_\alpha) = \sqrt{(F^{-1})_{\alpha\alpha}}$, F^{-1} being the inverse of the Fisher matrix. In order to focus on the role played by general relativity corrections, we have restricted the analysis to galaxy survey data, i.e. we have not included in the analysis forecasts from the on going Planck CMB experiment. We exploit here an enlarged version of the future Euclid galaxy survey experiment, with an area of 20000 deg², 24 redshift slices between $z = 0.15$ and $z = 2.55$ and a mean galaxy density of 1.56×10^{-3} , see Refs. [56, 57].

Two possible fiducial cosmologies are analyzed: i) a constant w cosmology (w denotes the dark energy equation of state), and ii) a constant w cosmology with the presence of primordial non Gaussianities (characterized by the parameter f_{NL}). In the analysis i), the model is described by the physical baryon and cold dark matter densities, $\Omega_b h^2$ and $\Omega_{\text{dm}} h^2$, the scalar spectral index, n_s , h , the dimensionless amplitude of the primordial curvature perturbations, A_s and w . In the analysis ii), which includes non-Gaussianities, the model is described by $\Omega_b h^2$, $\Omega_{\text{dm}} h^2$, h , w , the dark energy sound speed squared c_s^2 and the f_{NL} parameter. We have therefore fixed in this case the scalar spectral index and the dimensionless amplitude of primordial fluctuations, expected to be measured with excellent accuracy by the CMB Planck experiment. We follow a conservative approach, assuming that non-Gaussianities are constrained exclusively from the very large scale halo power spectrum.

In addition to the marginalized parameter errors, the biases induced in the cosmological parameters when data are wrongly fitted to the standard Newtonian power spectrum, neglecting general relativity corrections, are also computed. The biases in the cosmological parameters read [58]

$$\delta p_\alpha = (F^{-1})_{\alpha\beta} \sum_i \frac{\partial \mathcal{O}_{\text{obs}}^i}{\partial p_\beta} \frac{1}{\sigma_{\mathcal{O}_{\text{obs}}^i}^2} (\mathcal{O}_{\text{obs}}^i - \mathcal{O}_{\text{st}}^i) , \quad (31)$$

where the sum runs over the bins indices in $i = z, k$ and μ_k in the case of the 3-D power spectrum analysis, i.e. $\mathcal{O} = P(z, k, \mu_k)$, and $i = z$ and ℓ in the case of the 2-D power spectrum analysis, i.e. $\mathcal{O} = C_\ell(z)$. F is the Fisher matrix computed with the power spectra including general relativity corrections, $\mathcal{O}_{\text{obs}}^{(k,z)}$ and

$\mathcal{O}_{st}^{(k,z)}$ are the general relativity and standard Newtonian power spectra respectively and $\sigma_{\mathcal{O}_{obs}^i}$ is the error on the power spectrum with general relativity corrections.

In the case of analysis ii), we also have determined the shifts in the parameters $\{\Omega_b h^2, \Omega_{dm} h^2, h, w, c_s^2\}$ that would result when mock data generated with primordial non-Gaussianities ($f_{NL} = 20$ in this example) are fitted to a theoretical model without them. The idea is the following: if the data are fitted assuming a model M_1 with n_1 parameters, but the true underlying cosmology is a model M_2 characterized by n_2 parameters (with $n_2 > n_1$ and the parameter space of M_2 includes the model M_1 as a subset), the inferred values of the n_1 parameters will be shifted from their true values to compensate for the fact that the model used to fit the data is wrong. In the case illustrated here, M_2 will be the model *with* non-Gaussianities and M_1 the one *without* non-Gaussianities, i.e. with $f_{NL} = 0$. While the first n_1 parameters are the same for both models, the remaining $n_2 - n_1$ parameters in the enlarged model M_2 are accounting for the presence of non-Gaussianities, i.e. f_{NL} . Assuming a Gaussian likelihood, the shifts of the remaining n_1 parameters are given by [59]:

$$\delta\theta'_\alpha = -(G^{-1})_{\alpha\beta} F_{\beta\zeta} \delta\psi_\zeta \quad \alpha, \beta = 1 \dots n_1, \zeta = n_1 + 1 \dots n_2, \quad (32)$$

where G represents the Fisher sub-matrix for the model M_1 and F denotes the Fisher matrix for the model M_2 . In the case considered in this paper, M_1 is the model without primordial non-Gaussianities while $f_{NL} \neq 0$ in the model M_2 so that $n_2 - n_1 = 1$ and $\delta\psi = \delta f_{NL} = 20$.

B. 3-D Power Spectrum

For details regarding the calculation of the Fisher matrix for the 3-D power spectra $P(k, \mu_k)$ measured by a galaxy survey, see Ref. [60]. Here we perform a binning both in k and in μ_k , considering nine bins in the former quantity. The minimum scale k_{min} is fixed to $10^{-4} h/\text{Mpc}$ and the maximum scale is fixed to $0.1 h/\text{Mpc}$.

Table I contains the $1-\sigma$ marginalized errors on the cosmological parameters for analysis i), with a fiducial cosmology with constant dark energy equation of state $w = -1$. Two results are illustrated: those obtained with the standard Newtonian power spectrum and those obtained with general relativistic corrections included. Note that the errors obtained in the standard Newtonian prescription are generally 40% smaller than those obtained with general relativistic one, except for the w parameter in which case the tendency is reversed. The biases on the cosmological parameters are also presented in Tab. I. Note that their size is always smaller than the $1-\sigma$ marginalized errors and therefore these biases will barely interfere with the extraction of the cosmological parameters.

Table II presents the results from analysis ii), which includes non-Gaussianities with a fiducial $f_{NL} = 20$. Recently, the authors of Ref. [32] have shown that using methods to reduce the sampling variance and shot noise [61–63], a full sky galaxy survey can measure general relativistic effects. We do not exploit here these cancellation methods, leaving these combined techniques for a future study.

The errors on cosmological parameters resulting from the Fisher analysis are not improved including general relativity corrections. This fact was not unexpected, given that for the value of the f_{NL} considered in this analysis the changes in the power spectrum due to general relativity corrections are almost hidden by the effect of non-Gaussianities, see Sec. IIIB. Note also that the biases are always smaller than the corresponding $1-\sigma$ marginalized errors and therefore they will have no impact on the extraction of the cosmological parameters. Also, we find no significant shifts in the values of the cosmological parameters in any of the two prescriptions when the non-Gaussianity parameter f_{NL} is (wrongly) assumed to be zero. We conclude that relativistic corrections in the 3-D power spectrum will not help in constraining the cosmological parameters.

Finally, we briefly comment on the dependence of the cosmological parameter errors on the maximum scale considered in the analysis, k_{max} , assuming a fiducial cosmology with a constant dark energy equation of state $w = -1$. A larger k_{max} will imply a larger number of modes, more information from the location of the acoustic peaks is available and consequently the errors will be smaller. Figure 5 illustrates the size of the relative errors on the different cosmological parameters considered in analysis i) versus the scale k_{max} . Going from $k_{max} = 0.05 h/\text{Mpc}$ to $k_{max} = 0.2 h/\text{Mpc}$ the expected errors in $\Omega_b h^2, \Omega_{dm} h^2, h$ and w are reduced by a factor ~ 5 while in the case of the n_s parameter its error is reduced one order of magnitude.

Parameter	$P_{\Delta_{st}}(k, \mu_k)$	$P_{\Delta_{obs}}(k, \mu_k)$	Biases
$\Delta(\Omega_{dm}h^2)$	0.0035	0.0057	$7.0 \cdot 10^{-5}$
$\Delta(\Omega_b h^2)$	0.0010	0.0016	$-8.0 \cdot 10^{-5}$
ΔA_s	0.021	0.036	$1.1 \cdot 10^{-5}$
Δh	0.010	0.017	$1.3 \cdot 10^{-4}$
Δn_s	0.012	0.016	$-4.3 \cdot 10^{-3}$
Δw	0.015	0.010	$7.7 \cdot 10^{-3}$

TABLE I: $1-\sigma$ marginalized errors from the Euclid-like survey considered here for a fiducial cosmology with a constant dark energy equation of state, with a fiducial value $w = -1$. The third row illustrates the biases induced in the cosmological parameters when general relativistic corrections are (wrongly) neglected. The error on the amplitude of the primordial fluctuations ΔA_s is quoted in units of $2.64 \cdot 10^{-9}$.

Parameter	$P_{\Delta_{st}}(k, \mu_k)$	$P_{\Delta_{obs}}(k, \mu_k)$	Biases	Shifts
$\Delta(\Omega_{dm}h^2)$	$6.2 \cdot 10^{-4}$	$6.1 \cdot 10^{-4}$	$-4.8 \cdot 10^{-5}$	$-2.4 \cdot 10^{-4}$
$\Delta(\Omega_b h^2)$	$8.7 \cdot 10^{-4}$	$9.3 \cdot 10^{-4}$	$-6.3 \cdot 10^{-5}$	$3.4 \cdot 10^{-4}$
Δh	$3.5 \cdot 10^{-3}$	$3.8 \cdot 10^{-3}$	$-3.5 \cdot 10^{-4}$	$2.0 \cdot 10^{-3}$
Δw	$1.3 \cdot 10^{-2}$	$2.0 \cdot 10^{-3}$	$-3.5 \cdot 10^{-3}$	$1.5 \cdot 10^{-2}$
Δc_s^2	4.0	4.3	1.0	-2.5
Δf_{NL}	3.1	3.1	0.7	-

TABLE II: $1-\sigma$ marginalized errors from the Euclid-like survey considered here for a fiducial cosmology with a constant dark energy equation of state, with fiducial values $w = -1$, $f_{NL} = 20$ and $c_s^2 = 1$. The third row presents the biases induced in the cosmological parameters when general relativistic corrections are neglected. The shifts in the cosmological parameters when f_{NL} is set to zero but the data are generated with $f_{NL} = 20$ have been computed including general relativity corrections. Similar results are obtained using the standard Newtonian expression.

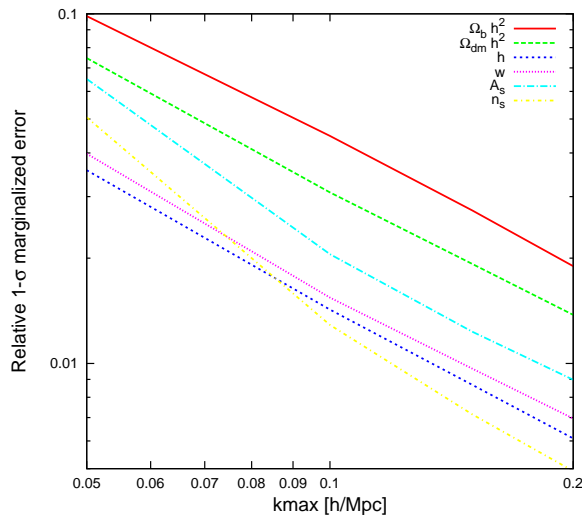


FIG. 5: Illustration of the relative $1-\sigma$ marginalized errors ($\Delta p/|p|$) dependence on the scale k_{max} using the standard Newtonian prescription for the cosmological parameters $p = \Omega_b h^2, \Omega_{dm} h^2, h, w, A_s$ and n_s for a fiducial cosmology with a constant dark energy equation of state with a fiducial value $w = -1$.

C. 2-D Angular Power Spectrum

The 2-D C_ℓ angular power spectrum is a projection of the 3-D quantity and therefore it implies an integration of the 3-D power spectrum $P(k)$ convoluted with a window function, the Bessel transform of the radial selection function, see Refs. [64, 65]. Therefore, the C_ℓ 's are not expected to give as much information on the cosmological parameters as the 3-D power spectrum $P(k)$. For the calculations presented here we have computed the C_ℓ assuming no magnification bias and a constant distribution of sources with redshift. For details regarding the calculation of the Fisher matrix for the 2-D power spectra measured by a galaxy survey, see Ref. [66] (notice that we considered $\ell_{min} = 2$ and $\ell_{max} = 400$).

Table III contains the $1-\sigma$ marginalized errors for analysis i), a fiducial cosmology with constant dark energy equation of state. We show the results when the Fisher matrix formalism is applied to the 2-D angular power spectrum in the standard Newtonian case and in the case in which general relativistic corrections are included. The errors in the two prescriptions are very similar. The biases in the cosmological parameters are also presented, and will have very little impact in the measurement of the cosmological parameters, as can be noticed from their sizes.

Table IV presents the analogous but for the analysis ii) with non-Gaussianities. Notice that the errors are exactly the same for the two prescriptions and therefore there is no improvement in the determination of the cosmological parameters when the general relativistic corrections are addressed in the angular power spectrum. The biases induced in the cosmological parameters when the data are fitted to the standard Newtonian power spectrum are also presented. These biases are always smaller than the corresponding $1-\sigma$ marginalized errors and therefore, will have no impact on the extraction of the cosmological parameters. Also, we find no significant shifts in the values of the cosmological parameters in any of the two prescriptions when the non-Gaussianity parameter f_{NL} is (wrongly) assumed to be zero. Consequently, from what regards the 2-D angular power spectrum, relativistic corrections will not have any impact on future measurements of the cosmological parameters, even if the information contained at the largest scales becomes at reach.

Notice that, as expected, the errors on the cosmological parameters obtained exploiting the 2-D power spectrum are, in general, larger than in the 3-D case. In the case of analysis i), the expected errors on w differ by one order of magnitude. The results of the 2-D and 3-D analysis should however roughly match in the limit of many narrow redshift bins. We have thus carried out a new fisher matrix analysis, decreasing the size of the redshift bin one order of magnitude in the 2-D analysis. In the latter case, similar marginalized errors are obtained when exploiting 2-D or 3-D power spectrum. In the case of the non-Gaussianity parameter f_{NL} the errors are three orders of magnitude larger when using the 2-D angular information. This is due to the fact that the 2-D C_ℓ angular power spectrum is essentially sensitive to modes transverse to the line of sight, while the 3-D $P(k)$ power spectrum benefit from extra information from the radial modes.

Parameter	$C_{\ell\Delta_{st}}$	$C_{\ell\Delta_{obs}}$	Biases
$\Delta(\Omega_{dm}h^2)$	0.0088	0.0086	0.003
$\Delta(\Omega_b h^2)$	0.002	0.002	$< 10^{-4}$
ΔA_s	0.093	0.093	-0.03
Δh	0.045	0.045	0.003
Δn_s	0.04	0.04	-0.02
Δw	0.24	0.24	0.01

TABLE III: $1-\sigma$ marginalized errors from the Euclid-like survey considered here for a fiducial cosmology with a constant dark energy equation of state with a fiducial value $w = -1$. The biases in the parameters are also presented. The error on the amplitude of the primordial fluctuations ΔA_s is quoted in units of $2.64 \cdot 10^{-9}$.

V. SUMMARY

The complete general relativistic description of the observed matter power spectrum at large scales is significantly different than the standard Newtonian one. The observed redshift and position of galaxies are

Parameter	$C_{\ell \Delta_{st}}$	$C_{\ell \Delta_{obs}}$	Biases	Shifts
$\Delta(\Omega_{dm}h^2)$	0.0106	0.0106	-0.0001	-0.00001
$\Delta(\Omega_b h^2)$	0.0053	0.0053	-0.0001	$< 10^{-6}$
Δh	0.0499	0.0499	-0.00004	$< 10^{-5}$
Δw	0.2276	0.2264	0.0006	-0.0007
Δc_s^2	4.886	4.771	-0.1527	0.025
Δf_{NL}	1870	1688	-1189	-

TABLE IV: $1-\sigma$ marginalized errors from the Euclid-like survey data for a fiducial cosmology with a constant dark energy equation of state, with fiducial values $w = -1$, $f_{NL} = 20$, $c_s^2 = 1$. The third row presents the biases induced in the cosmological parameters when general relativistic corrections are neglected. The shifts in the cosmological parameters when f_{NL} is set to zero but the data are generated with $f_{NL} = 20$ have been computed including general relativity corrections. Similar results are obtained using the standard Newtonian expression.

affected by the different matter fluctuations and by the gravity waves between the source galaxies and the observer, see Refs. [2–5]. In this paper we have studied the role of relativistic effects in the extraction of different cosmological parameters with the galaxy power spectrum measurements that will be available from future surveys.

We have explored the impact of such corrections in several cosmological scenarios as: constant (but $w \neq 1$) dark energy equation of state, time varying $w(a) = w_0 + w_a(1 - a)$ dark energy equation of state, coupled dark matter dark energy scenario, massive neutrinos and primordial non-Gaussianities. We have performed a Fisher matrix analysis considering data from a future Euclid-like spectroscopic galaxy survey for two scenarios: one with a constant dark energy equation of state, the other with non-Gaussianities. We find that general relativistic corrections will not interfere neither with the extraction of the standard cosmological parameters (as the cold dark matter and baryon densities) nor with the measurement of primordial non-Gaussianities. The expected marginalized errors when relativistic corrections are included in the matter or halo power spectra are very similar to those obtained in the standard Newtonian case. The biases induced in the different cosmological parameters when neglecting these relativistic effects are also negligible. We conclude that the measurement of the cosmological parameters will not be compromised by the presence of general relativistic effects, once they will be included in the analysis.

VI. ACKNOWLEDGMENTS

The authors would like to acknowledge R. de Putter, C. Peña Garay and L. Verde for very useful comments and enlightening discussions. O.M. is supported by AYA2008-03531 and the Consolider Ingenio-2010 project CSD2007-00060. L. L. H is supported in part by the IISN and by the Belgian Science Policy (IAP VI/11). S. Rigolin acknowledges the partial support of an Excellence Grant of Fondazione Cariparo and of the European Program Unification in the LHC era under the contract PITN- GA-2009-237920 (UNILHC).

Appendix A: Gauge invariant formalism

The conventions we use are from Ref. [67] with a few exceptions. More details can be found in Ref. [47]. For perturbations in a flat space time, the perturbation variables can be expanded by harmonic functions $Y^{(S)}(x, k)$ satisfying $(\nabla_x + k^2)Y^{(S)} = 0$. In the following we focus on scalar perturbations, for which we define:

$$Y_i^{(S)} = -\frac{1}{k}Y_{|i}^{(S)}, \quad (\text{A1})$$

$$Y_{ij}^{(S)} = \frac{1}{k^2}Y_{|ij}^{(S)} + \frac{1}{3}\gamma_{ij}Y^{(S)}. \quad (\text{A2})$$

Following Ref. [67], the FRW metric, up to first order in perturbation theory, can be written as:

$$g_{\mu\nu}dx^\mu dx^\nu = \bar{a}^2 \left[-(1 + 2A)d\tau^2 - 2B_i d\tau dx^i + (\gamma_{ij} + 2H_{ij})dx^i dx^j \right], \quad (\text{A3})$$

where γ_{ij} is the 3D flat metric with positive signature. The perturbations A , B_i and H_{ij} are functions of time and space and are in general gauge-dependent. Expanding the independent perturbations in the Fourier basis, and keeping only the scalar modes, we denote:

$$\begin{aligned} A &\rightarrow \tilde{A}Y^{(S)}; \\ B_i &\rightarrow \tilde{B}Y_i^{(S)}; \\ H_{ij} &\rightarrow \tilde{H}_L\gamma_{ij}Y^{(S)} + \tilde{H}_T Y_{ij}^{(S)}. \end{aligned}$$

In the following, for the sake of simplicity, we will omit the tilde symbols in the notation. Remember that all these quantities are represented by the correspondent Fourier expansion and depend only on time and on the 3-momentum k , while the position dependence is left only in the Y basis elements.

Using these metric perturbations, we can now define σ_g , the shear perturbation and \mathcal{R} , the curvature perturbation, as

$$\sigma_g = \frac{1}{k} \left(\dot{H}_T - kB \right); \quad (\text{A4})$$

$$\mathcal{R} = H_L + \frac{1}{3}H_T, \quad (\text{A5})$$

which are no gauge invariant quantities. The Bardeen metric gauge invariants are defined as [68]:

$$\Psi_B = A - \frac{\mathcal{H}}{k}\sigma_g - \frac{1}{k}\dot{\sigma}_g, \quad (\text{A6})$$

$$\Phi_B = H_L + \frac{1}{3}H_T - \frac{\mathcal{H}}{k}\sigma_g. \quad (\text{A7})$$

In the same line one can define perturbations for the energy-density for a given fluid a :

$$u_a^\mu = \frac{1}{\bar{a}} (1 - A, v_a^i); \quad (\text{A8})$$

$$T_a^{\mu\nu} = \bar{\rho}_a (1 + \delta_a) u_a^\mu u_a^\nu + \tau^{\mu\nu}, \quad (\text{A9})$$

where v_a^i is the peculiar velocity perturbation of the fluid and δ_a the fluid matter density contrast. Following [67] one define the following gauge-invariant quantities:

$$V_a = v_a - \frac{\dot{H}_T}{k}; \quad (\text{A10})$$

$$\Delta_a = \delta_a - \frac{\dot{\rho}_a}{\rho_a} \frac{\mathcal{R}}{\mathcal{H}}, \quad (\text{A11})$$

where Δ_a is the gauge invariant density contrast for the fluid a defined in the gravity rest frame. Notice that $v_a^i = v_a Y^i$ and that in Eq. (9) and the following, V^i refers to the gauge invariant velocity perturbation associated to the matter component, i.e. $V^i \equiv V_m^i = V_m Y^i$.

1. Photon wave vector: some relations

Here we provide several relations resulting from the null energy condition $K^\mu K_\mu = 0$ and the geodesic equations $K^\mu K_{;\mu}^\nu = 0$ useful in the derivation of the expression of gauge invariant matter density perturbation Δ_z defined in Eq. (7). On the one hand, from the perturbed null equation $K^\mu K_\mu = 0$, one obtains the following relation between the temporal and spatial null vector perturbations:

$$n^i \delta n_i = \frac{\delta\nu}{\nu} + (\Psi_B - \Phi_B) - \frac{1}{k^2} \frac{d}{d\lambda} \left(\frac{dH_T}{d\lambda} - 2H_T + kB \right), \quad (\text{A12})$$

where $d/d\lambda = \partial_\tau + n^i \partial_i$ and we have taken into account that the background null equation imposes $n^i n_i = 1$. We have also used the background geodesic equation giving rise to $n_i \partial_j n^i = n_i \dot{n}^i = 0$. On the other hand, the temporal geodesic equation $K^\nu K_{;\nu}^0$ gives the following condition:

$$\frac{d}{d\lambda} \left(\frac{\delta\nu}{\nu} + 2\Psi_B \right) = \left(\dot{\Psi}_B - \dot{\Phi}_B \right) - \frac{1}{k} \frac{d}{d\lambda} \left(\frac{d\sigma_g}{d\lambda} + 2\mathcal{H}\sigma_g \right). \quad (\text{A13})$$

2. Newtonian gauge

It can be useful for comparison to make a particular gauge choice. In the Newtonian gauge, $\sigma_g = 0$ and the perturbed metric is reduced to:

$$ds^2 = a^2 [-(1 + 2\Psi_N)d\tau^2 + (1 - 2\Phi_N)dx^i dx_i]. \quad (\text{A14})$$

In particular, for this gauge choice metric perturbations are given by:

$$\begin{aligned} \Psi_N &= \Psi_B = A, \\ \Phi_N &= -\Phi_B = -\mathcal{R}. \end{aligned} \quad (\text{A15})$$

The convergence κ , in the Newtonian gauge, reads:

$$\kappa = \int_0^{r_s} \frac{r_s - r}{2r_s r} \Delta_\Omega (\Phi_N + \Psi_N), \quad (\text{A16})$$

where r_s is the comoving distance between the source and the observer and $\Delta_\Omega = \cot\theta \partial_\theta + \partial_\theta^2 + 1/\sin^2\theta \partial_\phi^2$ is the angular laplacian on a unit sphere.

-
- [1] Camille Bonvin, Ruth Durrer, and M. Alice Gasparini. Fluctuations of the luminosity distance. *Phys. Rev.*, D73:023523, 2006, astro-ph/0511183.
 - [2] Jaiyul Yoo, A. Liam Fitzpatrick, and Matias Zaldarriaga. A New Perspective on Galaxy Clustering as a Cosmological Probe: General Relativistic Effects. *Phys. Rev.*, D80:083514, 2009, 0907.0707.
 - [3] Jaiyul Yoo. General Relativistic Description of the Observed Galaxy Power Spectrum: Do We Understand What We Measure? *Phys. Rev.*, D82:083508, 2010, 1009.3021.
 - [4] Camille Bonvin and Ruth Durrer. What galaxy surveys really measure. 2011, 1105.5280.
 - [5] Anthony Challinor and Antony Lewis. The linear power spectrum of observed source number counts. 2011, 1105.5292.
 - [6] Donghui Jeong, Fabian Schmidt, and Christopher M. Hirata. Large-scale clustering of galaxies in general relativity. 2011, 1107.5427.
 - [7] Rachel Mandelbaum, Uros Seljak, Guinevere Kauffmann, Christopher M. Hirata, and Jonathan Brinkmann. Galaxy halo masses and satellite fractions from galaxy-galaxy lensing in the sdss: stellar mass, luminosity, morphology, and environment dependencies. *Mon.Not.Roy.Astron.Soc.*, 368:715, 2006, astro-ph/0511164.
 - [8] <http://camb.info/sources/>.
 - [9] Michel Chevallier and David Polarski. Accelerating universes with scaling dark matter. *Int. J. Mod. Phys.*, D10:213–224, 2001, gr-qc/0009008.
 - [10] Eric V. Linder. Exploring the expansion history of the universe. *Phys.Rev.Lett.*, 90:091301, 2003, astro-ph/0208512.
 - [11] Andreas Albrecht, Gary Bernstein, Robert Cahn, Wendy L. Freedman, Jacqueline Hewitt, et al. Report of the Dark Energy Task Force. 2006, astro-ph/0609591.
 - [12] Eric V. Linder. The paths of quintessence. *Phys.Rev.*, D73:063010, 2006, astro-ph/0601052.
 - [13] Wayne Hu and Ignacy Sawicki. A Parameterized Post-Friedmann Framework for Modified Gravity. *Phys.Rev.*, D76:104043, 2007, 0708.1190.
 - [14] Wayne Hu. Parametrized Post-Friedmann Signatures of Acceleration in the CMB. *Phys.Rev.*, D77:103524, 2008, 0801.2433.
 - [15] Wenjuan Fang, Wayne Hu, and Antony Lewis. Crossing the Phantom Divide with Parameterized Post-Friedmann Dark Energy. *Phys. Rev.*, D78:087303, 2008, 0808.3125.

- [16] Marco Bruni et al. Disentangling non-Gaussianity, bias and GR effects in the galaxy distribution. 2011, 1106.3999.
- [17] D.S. Salopek and J.R. Bond. Nonlinear evolution of long wavelength metric fluctuations in inflationary models. *Phys.Rev.*, D42:3936–3962, 1990.
- [18] Alejandro Gangui, Francesco Lucchin, Sabino Matarrese, and Silvia Mollerach. The Three point correlation function of the cosmic microwave background in inflationary models. *Astrophys.J.*, 430:447–457, 1994, astro-ph/9312033.
- [19] Licia Verde, Li-Min Wang, Alan Heavens, and Marc Kamionkowski. Large scale structure, the cosmic microwave background, and primordial non-gaussianity. *Mon.Not.Roy.Astron.Soc.*, 313:L141–L147, 2000, astro-ph/9906301.
- [20] Eiichiro Komatsu and David N. Spergel. Acoustic signatures in the primary microwave background bispectrum. *Phys.Rev.*, D63:063002, 2001, astro-ph/0005036.
- [21] Daniel Babich, Paolo Creminelli, and Matias Zaldarriaga. The Shape of non-Gaussianities. *JCAP*, 0408:009, 2004, astro-ph/0405356.
- [22] Neal Dalal, Olivier Dore, Dragan Huterer, and Alexander Shirokov. The imprints of primordial non-gaussianities on large-scale structure: scale dependent bias and abundance of virialized objects. *Phys.Rev.*, D77:123514, 2008, 0710.4560.
- [23] Sabino Matarrese and Licia Verde. The effect of primordial non-Gaussianity on halo bias. *Astrophys.J.*, 677:L77–L80, 2008, 0801.4826.
- [24] Anze Slosar, Christopher Hirata, Uros Seljak, Shirley Ho, and Nikhil Padmanabhan. Constraints on local primordial non-Gaussianity from large scale structure. *JCAP*, 0808:031, 2008, 0805.3580.
- [25] Niayesh Afshordi and Andrew J. Tolley. Primordial non-gaussianity, statistics of collapsed objects, and the Integrated Sachs-Wolfe effect. *Phys.Rev.*, D78:123507, 2008, 0806.1046.
- [26] Carmelita Carbone, Licia Verde, and Sabino Matarrese. Non-Gaussian halo bias and future galaxy surveys. *Astrophys.J.*, 684:L1–L4, 2008, 0806.1950.
- [27] M. Grossi, L. Verde, C. Carbone, K. Dolag, E. Branchini, et al. Large-scale non-Gaussian mass function and halo bias: tests on N-body simulations. *Mon.Not.Roy.Astron.Soc.*, 398:321–332, 2009, 0902.2013.
- [28] Vincent Desjacques, Uros Seljak, and Ilian Iliev. Scale-dependent bias induced by local non-Gaussianity: A comparison to N-body simulations. 2008, 0811.2748.
- [29] Annalisa Pillepich, Cristiano Porciani, and Oliver Hahn. Universal halo mass function and scale-dependent bias from N-body simulations with non-Gaussian initial conditions. 2008, 0811.4176.
- [30] Carmelita Carbone, Olga Mena, and Licia Verde. Cosmological Parameters Degeneracies and Non-Gaussian Halo Bias. *JCAP*, 1007:020, 2010, 1003.0456.
- [31] David Wands and Anze Slosar. Scale-dependent bias from primordial non-Gaussianity in general relativity. *Phys.Rev.*, D79:123507, 2009, 0902.1084.
- [32] Jaiyul Yoo, Nico Hamaus, Uros Seljak, and Matias Zaldarriaga. Testing General Relativity on Horizon Scales and the Primordial non-Gaussianity. 2011, 1109.0998.
- [33] Tetsu Kitayama and Yasushi Suto. Formation rate of gravitational structures and the cosmic x-ray background radiation. *Mon.Not.Roy.Astron.Soc.*, 280:638, 1996, astro-ph/9602076.
- [34] Luca Amendola. Coupled quintessence. *Phys. Rev.*, D62:043511, 2000, astro-ph/9908023.
- [35] Luca Amendola. Perturbations in a coupled scalar field cosmology. *Mon. Not. Roy. Astron. Soc.*, 312:521, 2000, astro-ph/9906073.
- [36] Luca Amendola. Scaling solutions in general non-minimal coupling theories. *Phys. Rev.*, D60:043501, 1999, astro-ph/9904120.
- [37] Luca Amendola and Domenico Tocchini-Valentini. Stationary dark energy: the present universe as a global attractor. *Phys. Rev.*, D64:043509, 2001, astro-ph/0011243.
- [38] Luca Amendola. Linear and non-linear perturbations in dark energy models. *Phys. Rev.*, D69:103524, 2004, astro-ph/0311175.
- [39] Luca Amendola, Gabriela Camargo Campos, and Rogerio Rosenfeld. Consequences of dark matter - dark energy interaction on cosmological parameters derived from snia data. *Phys. Rev.*, D75:083506, 2007, astro-ph/0610806.
- [40] Jussi Valiviita, Elisabetta Majerotto, and Roy Maartens. Instability in interacting dark energy and dark matter fluids. *JCAP*, 0807:020, 2008, 0804.0232.
- [41] Jian-Hua He, Bin Wang, and Elcio Abdalla. Stability of the curvature perturbation in dark sectors’ mutual interacting models. *Phys. Lett.*, B671:139–145, 2009, 0807.3471.
- [42] Brendan M. Jackson, Andy Taylor, and Arjun Berera. On the large-scale instability in interacting dark energy and dark matter fluids. *Phys. Rev.*, D79:043526, 2009, 0901.3272.
- [43] M. B. Gavela, D. Hernandez, L. Lopez Honorez, O. Mena, and S. Rigolin. Dark coupling. *JCAP*, 0907:034, 2009, 0901.1611.
- [44] Gabriela Caldera-Cabral, Roy Maartens, and Bjoern Malte Schaefer. The Growth of Structure in Interacting Dark Energy Models. *JCAP*, 0907:027, 2009, 0905.0492.
- [45] Jussi Valiviita, Roy Maartens, and Elisabetta Majerotto. Observational constraints on an interacting dark energy model. 2009, 0907.4987.

- [46] Elisabetta Majerotto, Jussi Valiviita, and Roy Maartens. Adiabatic initial conditions for perturbations in interacting dark energy models. 2009, 0907.4981.
- [47] M. B. Gavela, L. Lopez Honorez, O. Mena, and S. Rigolin. Dark Coupling and Gauge Invariance. *JCAP*, 1011:044, 2010, 1005.0295.
- [48] Laura Lopez Honorez, Beth A. Reid, Olga Mena, Licia Verde, and Raul Jimenez. Coupled dark matter-dark energy in light of near Universe observations. *JCAP*, 1009:029, 2010, 1006.0877.
- [49] Matteo Martinelli, Laura Lopez Honorez, Alessandro Melchiorri, and Olga Mena. Future CMB cosmological constraints in a dark coupled universe. 2010, 1004.2410.
- [50] Laura Lopez Honorez, Olga Mena, and Grigoris Panotopoulos. Higher-order coupled quintessence. *Phys.Rev.*, D82:123525, 2010, 1009.5263.
- [51] E. Komatsu et al. Seven-Year Wilkinson Microwave Anisotropy Probe (WMAP) Observations: Cosmological Interpretation. 2010, 1001.4538.
- [52] Chung-Pei Ma and Edmund Bertschinger. Cosmological perturbation theory in the synchronous and conformal Newtonian gauges. *Astrophys. J.*, 455:7–25, 1995, astro-ph/9506072.
- [53] Max Tegmark, Andy Taylor, and Alan Heavens. Karhunen-Loeve eigenvalue problems in cosmology: How should we tackle large data sets? *Astrophys.J.*, 480:22, 1997, astro-ph/9603021.
- [54] Gerard Jungman, Marc Kamionkowski, Arthur Kosowsky, and David N. Spergel. Cosmological parameter determination with microwave background maps. *Phys.Rev.*, D54:1332–1344, 1996, astro-ph/9512139.
- [55] Ronald Aylmer Fisher. The Fiducial Argument in Statistical Inference. *Annals Eugen.*, 6:391–398, 1935.
- [56] A. Refregier, O. Boulade, Y. Mellier, B. Milliard, R. Pain, et al. DUNE: The Dark Universe Explorer. 2006, astro-ph/0610062.
- [57] A. Refregier, A. Amara, T.D. Kitching, A. Rassat, R. Scaramella, et al. Euclid Imaging Consortium Science Book. 2010, 1001.0061.
- [58] Roland de Putter and Eric V. Linder. To Bin or Not To Bin: Decorrelating the Cosmic Equation of State. *Astropart.Phys.*, 29:424–441, 2008, 0710.0373.
- [59] Alan F. Heavens, T. D. Kitching, and L. Verde. On model selection forecasting, Dark Energy and modified gravity. *Mon. Not. Roy. Astron. Soc.*, 380:1029–1035, 2007, astro-ph/0703191.
- [60] Hee-Jong Seo and Daniel J. Eisenstein. Probing dark energy with baryonic acoustic oscillations from future large galaxy redshift surveys. *Astrophys.J.*, 598:720–740, 2003, astro-ph/0307460.
- [61] Uros Seljak. Extracting primordial non-gaussianity without cosmic variance. *Phys.Rev.Lett.*, 102:021302, 2009, 0807.1770.
- [62] Uros Seljak, Nico Hamaus, and Vincent Desjacques. How to suppress the shot noise in galaxy surveys. *Phys.Rev.Lett.*, 103:091303, 2009, 0904.2963.
- [63] Nico Hamaus, Uros Seljak, and Vincent Desjacques. Optimal Constraints on Local Primordial Non-Gaussianity from the Two-Point Statistics of Large-Scale Structure. 2011, 1104.2321.
- [64] Dragan Huterer, Lloyd Knox, and Robert C. Nichol. The Angular power spectrum of EDSGC galaxies. *Astrophys.J.*, 555:547, 2001, astro-ph/0011069.
- [65] Max Tegmark et al. The Angular power spectrum of galaxies from Early SDSS Data. *Astrophys.J.*, 571:191–205, 2002, astro-ph/0107418.
- [66] Wayne Hu and Bhuvnesh Jain. Joint galaxy - lensing observables and the dark energy. *Phys.Rev.*, D70:043009, 2004, astro-ph/0312395.
- [67] Hideo Kodama and Misao Sasaki. Cosmological Perturbation Theory. *Prog. Theor. Phys. Suppl.*, 78:1–166, 1984.
- [68] James M. Bardeen. Gauge Invariant Cosmological Perturbations. *Phys. Rev.*, D22:1882–1905, 1980.